

# Nutrient Restriction Improves the Therapeutic Efficacy of Sorafenib by Inducing Ferroptosis via the NRF2/HO-1/GPX4 Pathway in Hepatocellular Carcinoma

Xinxin Chen<sup>1,\*</sup>, Ke Chen<sup>1,\*</sup>, Zhengye Xu<sup>1</sup>, Kelin Shou<sup>1</sup>, Chong Jin<sup>2</sup>, Zhencang Zheng<sup>3</sup>, Kan Chen<sup>1</sup>

<sup>1</sup>College of Life Sciences and Medicine, Zhejiang Sci-Tech University, Hangzhou, 310018, People's Republic of China; <sup>2</sup>Department of General Surgery, Taizhou Central Hospital, Taizhou University Hospital, Taizhou, Zhejiang, 318000, People's Republic of China; <sup>3</sup>Department of Critical Care Medicine, Taizhou Central Hospital, Taizhou University Hospital, Taizhou, Zhejiang, 318000, People's Republic of China

\*These authors contributed equally to this work

Correspondence: Zhencang Zheng, Department of Critical Care Medicine, Taizhou Central Hospital, Taizhou University Hospital, Taizhou, Zhejiang, 318000, People's Republic of China, Email [zcc2448909@163.com](mailto:zcc2448909@163.com); Kan Chen, College of Life Sciences and Medicine, Zhejiang Sci-Tech University, Hangzhou, 310018, People's Republic of China, Email [chenkan@zstu.edu.cn](mailto:chenkan@zstu.edu.cn)

**Background and Aims:** Hepatocellular carcinoma (HCC) is a prevalent malignant tumor with a high fatality rate, making it imperative to explore novel therapeutic approaches. This study aimed to assess the effectiveness and underlying mechanism of nutrient restriction in potentiating Sorafenib-induced cell death.

**Methods:** Cell viability was measured using MTT assays. Mitochondrial membrane potential (MMP) was assessed by the JC-1 probes. The levels of Reactive oxygen species (ROS) were determined using a DCFH-DA probe. Lipid peroxidation was quantified using the C11-BODIPY probe and a malondialdehyde (MDA) kit. Intercellular Fe<sup>2+</sup> was assessed using the FerroOrange probe. Western blot, HE staining, and immunohistochemistry (IHC) techniques were utilized to analyze the impact of combination therapy on NRF2, HO-1, and GPX4 proteins. Nude mice xenograft models were established to evaluate the inhibitory effects of the combination therapy in vivo.

**Results:** Nutrient restriction/Intermittent fasting enhanced Sorafenib-induced cell death both in vivo and in vitro by elevating ROS and MDA levels, promoting excessive lipid peroxidation, and increasing intercellular Fe<sup>2+</sup> accumulation. Notably, key ferroptosis-associated proteins, including NRF2, GPX4, and HO-1, were significantly down-regulated by combination treatment, while glutathione (GSH) supplementation reversed this downregulation.

**Conclusion:** The combination of nutrient restriction and Sorafenib significantly enhanced anti-tumor efficacy both in vivo and in vitro. Mechanistically, nutrient restriction potentiated Sorafenib-induced ferroptosis via the NRF2/HO-1/GPX4 pathway in HCC cells.

**Keywords:** ferroptosis, hepatocellular carcinoma, intermittent fasting, nutrient restriction, sorafenib

## Introduction

Hepatocellular carcinoma (HCC) is the main form of primary liver cancer, which represents a widespread and deadliest malignant tumor.<sup>1</sup> Despite notable progress in therapeutic approaches, HCC remains characterized by its poor prognosis and resistance to chemotherapy. Currently, Sorafenib and Lenvatinib are the two first-line systemic medications available for treating advanced HCC.<sup>2</sup> However, the survival advantages of these drugs are only moderate.<sup>3,4</sup> Consequently, the urgency to explore a highly efficacious treatment with minimal side effects has escalated significantly.<sup>5</sup>

Alterations in the nutritional metabolism trigger metabolic reprogramming in tumor cells, ultimately heightening their sensitivity to external stimuli.<sup>6</sup> Recently, dietary interventions, particularly nutrient restriction, have emerged as a potential adjunct to conventional cancer therapies.<sup>7,8</sup> Presently, more than 10 clinical trials are evaluating the safety and efficacy of fasting-mimicking diets in combination with various anticancer drugs (<http://clinicaltrials.gov>).

Nevertheless, the precise mechanisms underlying these dietary therapies remain poorly understood. A study revealed that intermittent fasting activates the AMPK signaling pathway, leading to mitochondrial restructuring.<sup>9</sup> By utilizing UMI-mRNA sequencing, Liu et al identified ferroptosis as the most significantly influenced pathway by fasting.<sup>10</sup> Thus, they posited that the combination of fasting and ferroptosis-inducer could lead to tumor suppression and elimination. Ferroptosis is a form of regulated cell death triggered by the accumulation of iron, the production of reactive oxygen species (ROS), and the ensuing process of lipid peroxidation.<sup>11</sup>

Emerging evidence implicates ferroptosis in the pathogenesis and therapy resistance of HCC. More recently, studies have revealed that Sorafenib, a standard therapy known to induce apoptosis, also exerts its cytotoxic effects in HCC by triggering ferroptosis.<sup>12–14</sup> This mechanism is further supported by studies demonstrating that suppression of ferroptosis promotes radioresistance in HCC.<sup>15</sup> At the molecular level, nuclear factor erythroid 2-related factor 2 (NRF2), a key regulator of ferroptosis, is activated in HCC via the IKK $\beta$ /NF- $\kappa$ B-inducible protein SQSTM1/p62.<sup>16</sup> Consistently, Maeda et al observed that enhanced DEN-induced hepatocarcinogenesis correlated with elevated lipid peroxidation and cell death, reversibly blocked by the glutathione precursor NAC.<sup>17,18</sup> Collectively, these findings position ferroptosis induction as a promising therapeutic strategy.

In this study, we investigated the anti-tumor efficacy of nutrient restriction/intermittent fasting combined with Sorafenib. Furthermore, we probed into the underlying mechanism of this combination therapy to restrain HCC progression, as well as its influence on mitochondrial function and ferroptosis. The aim of the present study was to develop a conceptual foundation for the treatment of HCC, and thus foster the researches for novel pharmaceutical agents.

## Materials and Methods

### Reagents

The high/low-glucose DMEM mediums were acquired from Gibco (Shanghai, China. Cat. No. BC-M-005). Sorafenib and Lenvatinib were purchased from Selleck Chemicals (Shanghai, China. Cat. No., S7397; S1164). MTT was purchased from Biofrox (Cat. No. 1334GR005). MDA kit, ATP kit, NADP+/NADPH colorimetric kit, and fluorescent probes including the JC-1 and the FerroOrange were purchased from Beyotime Biotechnology (Shanghai, China. Cat. No. S0131S; S0026; S0179). The ROS kit was bought from Solarbio (Beijing, China. Cat. No. CA1410), while the C11-BODIPY probe was acquired from Dojindo (Beijing, China. Cat. No. L2678). Glutathione (GSH) was purchased from MACKLIN (Shanghai, China. Cat. No. R917465).

### Cell Culture

The human HCC cell line Huh7 (RRID: CVCL\_0336) and PLC/PRF/5 (RRID: CVCL\_0485) were purchased from Meisen CTCC (Hangzhou, China). Cells were confirmed mycoplasma free. The cells were cultured in a high-glucose DMEM medium and low-glucose DMEM medium. The high-glucose DMEM medium containing 25 mM D-glucose with 10% FBS (Hyclone) (GM medium: Growth Medium). Otherwise, cells were cultured in a low-glucose DMEM medium containing 5.5mM D-glucose with 5% FBS (SM medium: Starvation Medium). The SM parameters were designed to physiologically mimic conditions.<sup>8</sup> Both mediums were supplemented with 4 mM L-glutamine and 50 units/mL penicillin-streptomycin (Solarbio. Cat. No. P1410). Cells were incubated at 37°C in a humidified atmosphere containing 5% CO<sub>2</sub>.

### Cell Viability Assay

The MTT assay was utilized to assess cell viability. Cells were seeded into 96-well plates at a density of  $5 \times 10^3$  cells per well. Drugs were dissolved in DMSO and diluted in PBS to final DMSO concentrations  $\leq 0.05\%$  (v/v). Then serial dilutions of Sorafenib (2.5, 5, 10, and 20  $\mu$ M) or Lenvatinib (5, 10, 25, and 50  $\mu$ M) were added, and the controls received of PBS containing equivalent DMSO concentrations at equal volume. After 48h drug exposure (ample time to observe dynamic changes in cell viability post-drug treatment),<sup>19</sup> cells were incubated with MTT reagent (5 mg/mL) for 4h at 37°C. Formazan crystals were solubilized in 150  $\mu$ L DMSO. The absorbance was determined at 490 nm wavelength by using a microplate reader (Thermo Fisher, MA). For the calculation of IC<sub>50</sub> values, The percentage of cell viability relative to the untreated control group was calculated for each concentration. These viability data were then plotted

against the corresponding logarithmic concentrations of the compound. The IC<sub>50</sub> value was determined using GraphPad Prism software via non-linear regression analysis, which generates the concentration of the compound that inhibits cell viability by 50%.

### Assessment of Mitochondrial Membrane Potential (MMP)

The MMP evaluation was conducted using the JC-1 fluorescent probe. After rinsing the cells with PBS, they were incubated in a JC-1 staining solution diluted at 1:2000. Subsequently, the cells were incubated at 37 °C for 20 mins. Finally, the cells were rinsed with PBS and subjected to analysis using a flow cytometer (FCM) (AccuriC6, BD Biosciences). The data from FCM was processed using FlowJo™ V10.8 Software.

### Measurement of Reactive Oxygen Species (ROS)

ROS levels were assessed by utilizing the DCFH-DA fluorescent probe, a cell-permeable compound commonly employed for ROS detection.<sup>12</sup> Cells were seeded in 6-well plates at a density of  $5 \times 10^4$  cells per well and treated with drugs for 24 hours. The cells were incubated with 1 mL of DCFH-DA (diluted 1:10000 with PBS) for 3 mins at 37 °C in the dark. Subsequently, cells were rinsed 3 times with washing buffer to remove extracellular probe. Finally, cells were collected and the fluorescent signals were measured immediately using FCM (Ex: 480 nm/Em: 525–530 nm).

### Assessments of Malondialdehyde (MDA) and Lipid Peroxidation

MDA was determined using dedicated assay kits. Cells were plated in 6-well dishes at a concentration of  $5 \times 10^4$ /well and exposed to drugs for 24 hours (in ferroptotic events, MDA elevation precede cell death, peaking 16–24 hours post-stimulation).<sup>20</sup> The MDA assay was performed according to the manufacturer's instructions. Lipid peroxidation was assessed by utilizing the C11-BODIPY probe. Cells were rinsed with PBS and subsequently incubated with a 10 μM C11-BODIPY solution at 37 °C for 20 mins. Finally, fluorescence was examined through FCM.

### Detection of Fe<sup>2+</sup>

The Fe<sup>2+</sup> was measured by employing the FerroOrange fluorescent probe. Initially, cells were incubated with drugs for 24 hours (during ferroptosis, accumulated Fe<sup>2+</sup> occur before cell death, reaching their highest levels 16–24 hours after stimulation).<sup>20</sup> Upon rinsing with PBS, the cells were suspended with 1 μM FerroOrange working solution and maintained at 37 °C in dark for 30 mins. Finally, fluorescent microscopy was utilized to observe and capture images.

### Assessment of ATP and NADP+/NADPH

Following cell adhesion and treatment, the cells were lysed, and samples were subsequently collected. The levels of ATP and MDA were assessed utilizing specialized assay kits according to the manufacturer's introduction. NADP+ and NADPH were determined by employing the NADP+/NADPH quantification colorimetric kit. Colorimetric measurements were performed at 450 nm using a Hidex Sense plate reader (MULTISKAN sky, Thermo).

### Xenograft Tumor in Nude Mice

Xenograft tumor models were established in nude mice using a protocol approved by the Animal Ethics and Welfare Committee of Zhejiang Sci-Tech University. Specific pathogen-free (SPF) female Balb/c nude mice (6–7 weeks old, initial body weight 18–20 g) were procured from Slack Laboratory Animal Co., Ltd. (Production License: SCXK [Hu] 2017-0005; Quality Certificate: 20220004046355). The body weight variation range was 19.2–21.3 g (mean ± SD: 20.1 ± 0.6 g) prior to group randomization. These mice were accommodated in groups of 4 per cage, maintained at a temperature range of 18–23 °C. After 3 days of adaptive culture, subcutaneous inoculation of  $5 \times 10^6$  Huh7 cells. The cells were injected subcutaneously into the axillary region of the mice. On the 7th day after inoculating tumor-bearing mice, those with established xenograft tumors were randomly divided into four groups, with 6 mice in each group: ad libitum (AL) group, intermittent fasting (IF) group, AL treated with Sorafenib group (AL+Sora), and IF treated with Sorafenib group (IF+Sora). In the AL group, mice had free access to food and water, whereas in the IF group, food and water were withdrawn for 16 hours every day (16:8 diet). The mice received either consecutive gastric gavage of Sorafenib or an equal volume of saline. Mice were administered Sorafenib at

5mg/kg tiw (three times a week) for 5 weeks. Tumor volumes were calculated every weekly using the formula: length  $\times$  (width)<sup>2</sup>  $\times$  0.5. At week 5 post-grouping (Day 42 post-inoculation), the mice were anesthetized using 4% isoflurane United States Pharmacopoeia (USP) 100%. They were then sacrificed by rapid cervical dislocation, with death confirmed when breathing and heartbeat stopped. Tumors were immediately isolated and weighed. One portion of the tumor was fixed in 4% paraformaldehyde; the remainder was stored in liquid nitrogen for further analysis. All animal procedures performed in this study were approved by the Institute Animal Care and Use Committee (IACUC) of Zhejiang Sci-Tech University (Approval No: IACUC-20190108; Approval Date: March 2019) (Environment License No: SYXK [Zhe] 2021-0001), and conducted in compliance with the GB/T 35892-2018 (Guideline for ethical review of animal welfare) and reported of In Vivo Experiments (ARRIVE) guidelines.

## Western Blot

Protein samples were isolated and quantified using the BCA kit (Vazyme, Nanjing, China. Cat. No. E112-02). Subsequently, the proteins were separated via electrophoresis using 12% SDS-PAGE gels. The membranes were incubated with primary antibodies overnight at 4 °C and GAPDH was used as a loading control. Subsequently, the membranes were incubated with secondary antibodies at a dilution of 1:5000 for one hour. For visualization, an ECL detecting kit (ABclonal, WuHan, China. Cat. No. RM00021p) and an imaging system (Clinx 6000EXP, Shanghai, China) were employed. Band intensities were measured using ImageJ software normalized to loading controls.<sup>21</sup> Three independent cell cultures for cell-based Western blot assay, and three individual animals for tissue-based Western blot analysis. The antibodies used in this study are listed in [Supplementary Table 1](#).

## HE and Immunohistochemistry (IHC) Staining

The tumors were fixed in 4% paraformaldehyde. After undergoing a series of steps including dehydration, clearing, and embedding in paraffin, 4  $\mu$ m tumor sections were acquired. These sections were stained with hematoxylin for 3 mins and eosin for another 5 mins. For IHC, the paraffin-embedded sections were deparaffinized and rehydrated through a graded series of ethanol. Antigen retrieval was facilitated using citrate buffer, and endogenous peroxidase activity was blocked with 3% hydrogen peroxide. The sections were subsequently incubated with anti-GPX4 at 4 °C overnight, followed by incubation with an HRP-labeled secondary antibody respectively. DAB chromogen solution was applied for visualization. Microscopic images were acquired using K-Viewer software.

## Statistical Analysis

Data are presented as mean  $\pm$  SD. The comparisons were performed with the Student's *t* test between two groups. One-way ANOVA with Tukey's post-hoc test was used for comparing three or more groups.  $p < 0.05$  was considered as statistically significance.

## Results

### Nutrient Restriction Significantly Boosted the Anti-Tumor Effect of Sorafenib in HCC

To investigate whether nutrient restriction can enhance the anti-tumor efficacy of drugs against HCC, we mimicked nutrient restriction by culturing cells in a low-glucose medium containing relative low serum. Using MTT assay, we assessed the responsiveness of HCC cells to two first-line HCC medications, Sorafenib and Lenvatinib, in high-glucose (GM medium) or low-glucose (SM medium) medium. Our findings indicated that cells cultivated in the SM medium exhibited heightened sensitivity to the drugs ([Figure 1A–D](#)). Following treatment in the GM medium, the IC<sub>50</sub> values for Sorafenib were 25.70  $\mu$ M for Huh7 and 18.19  $\mu$ M for PLC/PRF/5. Remarkably, these values decreased to 5.24  $\mu$ M for Huh7 and 4.89  $\mu$ M for PLC/PFR/5 when cultured in the SM medium. In the case of Lenvatinib, the IC<sub>50</sub> values decreased from 14.12  $\mu$ M for Huh7 and 30.10  $\mu$ M for PLC/PRF/5 in the GM medium, to 6.16  $\mu$ M and 19.49  $\mu$ M, respectively ([Table 1](#)). Notably, the relative potency of the two drugs differed between the cell lines, suggesting possible differences in their dependency on specific signaling pathways.

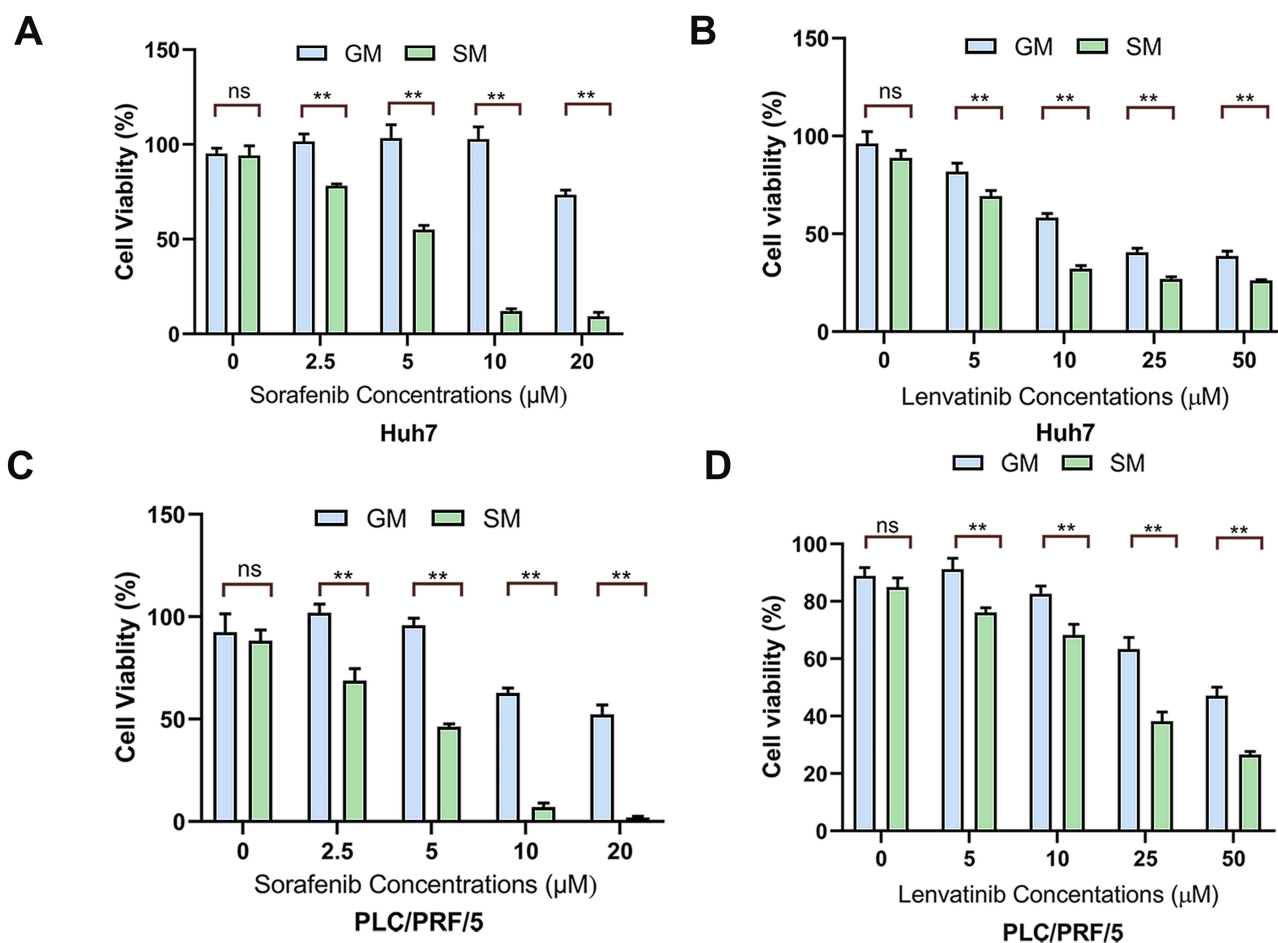


**Figure 1** Nutrient restriction significantly enhanced the anti-tumor effects of drugs in HCC. (**A** and **B**) Sorafenib and Lenvatinib potently suppressed the proliferation of Huh7 cells grown in SM medium, as assessed by the MTT assay (mean  $\pm$  SD,  $n = 6$ , ns, not significant,  $**p < 0.01$ ); (**C** and **D**) Sorafenib and Lenvatinib significantly reduced the growth of PLC/PRF/5 cells in SM medium, as assessed by the MTT assay (mean  $\pm$  SD,  $n = 6$ ,  $**p < 0.01$ ). GM: Growth Medium (high-glucose DMEM supplemented with 10% FBS); SM: Starvation Medium (5.5 mM-glucose DMEM supplemented with 5% FBS); Sora: Sorafenib. Shown is a result from at least 3 independent experiments.

Given the significant effect on cell sensitivity and minimal cytotoxicity observed with 5  $\mu$ M Sorafenib (by up to 40–50% in SM medium of Huh7 and PLC/PRF/5 cells,  $p < 0.01$ ), this concentration was selected. Moreover, considering Sorafenib's greater sensitivity to nutrient restriction compared to Lenvatinib, it was chosen for subsequent in vivo experiments.

## Nutrient Restriction Enhanced Sorafenib's Effect on Mitochondria Injury

Sorafenib, a multi-kinase inhibitor targeting tyrosine kinase, can effectively prevent tumor cell proliferation by interrupting the RAS/RAF/MEK/ERK signaling pathway.<sup>13,14</sup> To investigate the mechanisms of action of the combined

**Table 1** Drug IC50 Values

IC 50 ( $\mu$ M)	Huh7 Cell Line		PLC/PRF/5 Cell Line	
	Sorafenib	Lenvatinib	Sorafenib	Lenvatinib
GM medium	25.70	14.12	18.19	30.10
SM medium	5.24	6.16	4.89	19.49

**Notes:** GM: Growth Medium (high-glucose DMEM supplemented with 10% FBS); SM: Starvation Medium (5.5 mM-glucose DMEM supplemented with 5% FBS); IC50: half maximal inhibitory concentration; Sora: Sorafenib. Shown is a result from at least 3 independent experiments.

treatment, we examined the expression and activation of ERK, a crucial downstream component in the RAF/MEK/ERK pathway. The results showed that nutritional restriction attenuated ERK activation (Figure 2A). Subsequently, we conducted Western blot to examine the impact of the combined treatment on the cell apoptotic pathway. The results demonstrated that Sorafenib, nutrient restriction alone, or their combination did not significantly change the expression of those apoptotic-associated proteins (Figure 2B). This implies that the observed cell death is independent on the classical apoptotic pathway, which is in line with previous research indicating that the efficacy of Sorafenib is not related to cell apoptosis.<sup>22</sup>

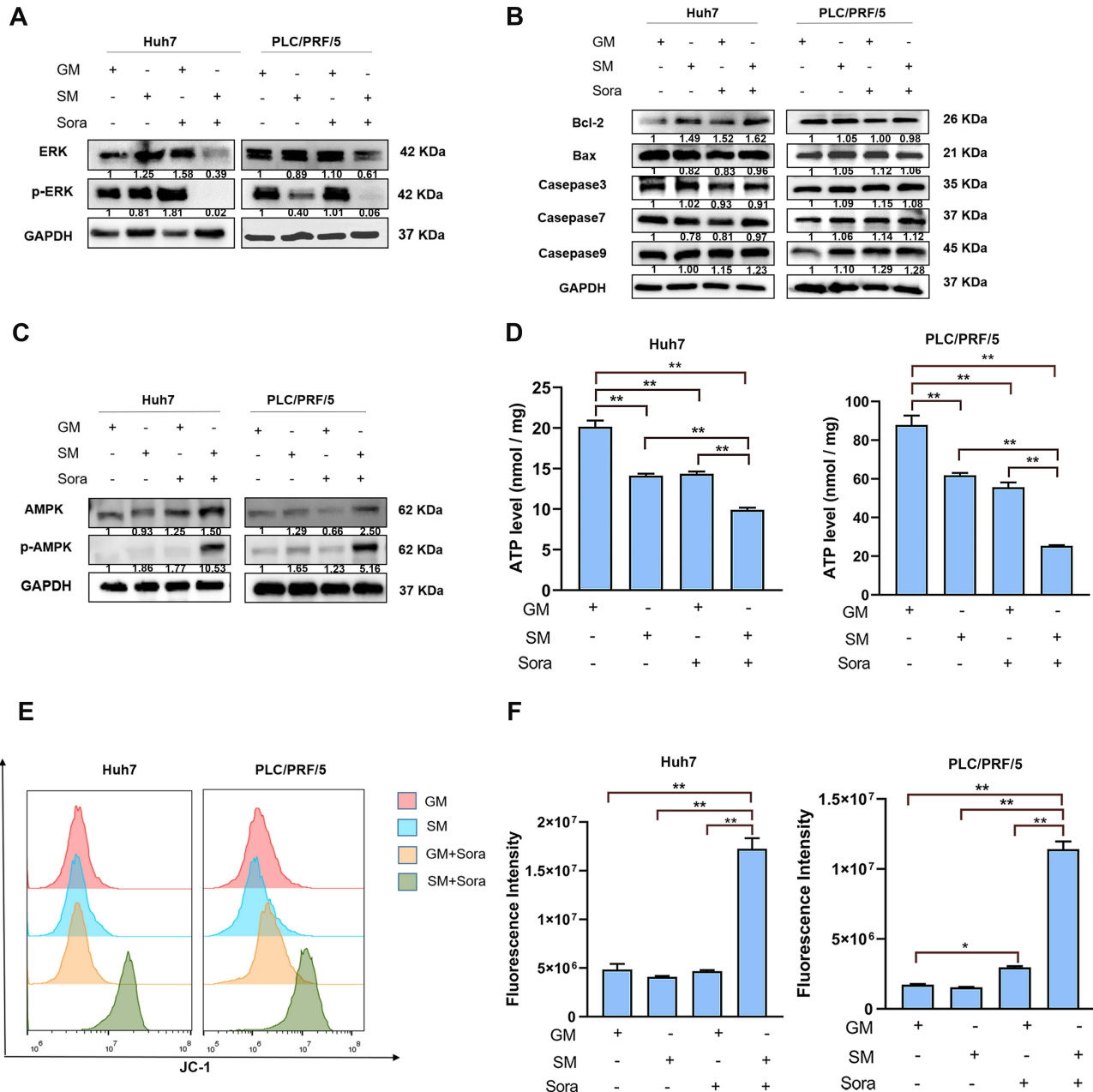


**Figure 2** The combination of nutrient restriction and Sorafenib disrupted the energy balance in HCC cells. **(A)** Western blot revealed changes in the expression and activation of ERK; **(B)** Western blot analysis of various anti-apoptotic and pro-apoptotic proteins; **(C)** Western blotting revealed changes in the expression and phosphorylation of AMPK; **(D)** Measurement of cellular ATP levels indicated a significant alteration (mean ± SD, n = 6, \*\*p < 0.01); **(E)** The combination treatment significantly reduced the cell's MMP; **(F)** Quantification of cell MMP. Shown is a result from at least 3 independent experiments (mean ± SD, n = 6, \*p < 0.05; \*\*p < 0.01). **Abbreviation:** MMP, mitochondrial membrane potential.

Furthermore, we probed into whether nutritional restriction disrupted the energy balance in HCC cells. AMP-activated protein kinase (AMPK), an energy sensor,<sup>23</sup> plays pivotal roles in growth regulation and metabolic reprogramming.<sup>24</sup> AMPK becomes activated when intracellular ATP levels drop. Therefore, ATP levels and AMPK expression were detected in this research. Our results revealed that both nutritional restriction and Sorafenib alone were capable of reducing cellular ATP levels. Notably, phosphorylated AMPK was obviously increased in the cells treated by the combination (Figure 2C). Correspondingly, their combination manifested a synergistic effect in lowering ATP (Figure 2D). These observations demonstrate that the combination treatment impairs ATP generation.

Mitochondria acts as the primary subcellular organelles for energy production, and mitochondrial membrane potential (MMP) serves as a key hallmark of cell energy conversion. By employing the JC-1 fluorescent probe, the changes in MMP can be detected through the shift from red fluorescence (polymer) to green fluorescence (monomer), and the degree of mitochondrial depolarization is determined by the ratio of fluorescence intensity. Our results revealed a significant increase in the percentage of JC-1 monomer in cells treated by the combination (3.6-fold in Huh7, 6.6-fold in PLC/PRF/5;  $p < 0.01$ , Figure 2E and F), suggesting that nutrient restriction enhanced Sorafenib's injury to mitochondria.

## The Combination of Sorafenib and Nutrient Restriction Disrupted the Redox Balance in HCC Cells

Nicotinamide adenine dinucleotide (NAD<sup>+</sup>/NADH) and nicotinamide adenine dinucleotide phosphate (NADP<sup>+</sup>/NADPH) redox couples are essential for maintaining cellular redox homeostasis.<sup>25</sup> Imbalances or deficiencies in these redox couples have been associated with various pathological disorders, often leading to excessive production of ROS due to oxidative stress. To explore if nutritional restriction disrupted the redox balance in HCC cells, we assessed the levels of NADP<sup>+</sup> and NADPH in these cells. We found a significant decrease in the NADP<sup>+</sup>/NADPH ratio upon treatment with either Sorafenib or nutritional restriction (1.2-fold and 1.6-fold reductions in Huh7 cells,  $p < 0.05$ ; 1.4-fold and 3.1-fold reductions in PLC/PRF/5 cells,  $p < 0.01$ ). Particularly, the NADP<sup>+</sup>/NADPH ratio dropped below 0.1 in combined treated cells, indicating a profound redox imbalance (6.9-fold decrease in Huh7 and 6.4-fold decrease in PLC/PRF/5 cells vs GM control,  $p < 0.01$ , Figure 3A).

ROS are by-products of multiple cellular processes. Under normal conditions, they serve as signal transducers regulating physiological activities. However, once ROS levels surpass the cell's endogenous antioxidant capacity, the redox balance is disrupted, ultimately leading to cell death.<sup>26</sup> The combined effect of Sorafenib and nutritional restriction on MMP reduction and redox imbalance prompted us to explore cellular ROS levels. DCFH-DA, a common probe for detecting specific ROS types, including superoxide or hydroxyl radicals, was utilized. Our findings revealed a significant increase in fluorescence intensity in the combination group (2.9-fold in Huh7 and 3.8-fold in PLC/PRF/5 cells,  $p < 0.01$ , Figure 3B and C).

Malondialdehyde (MDA) is a frequently utilized indicator of lipid peroxidation.<sup>20,27</sup> Through measuring MDA within cells, we found that the combined treatment prominently enhanced MDA levels (2.3-fold in Huh7 and 1.9-fold in PLC/PRF/5 cells,  $p < 0.01$ , Figure 3D). Collectively, the above findings suggest that nutrient restriction and Sorafenib synergistically disrupted redox balance, thereby causing excessive ROS production in HCC cells and resulting in ROS-dependent cell death.

## Nutrient Restriction Enhanced the Efficacy of Sorafenib by Inducing Ferroptosis via the NRF2/HO-1/GPX4 Axis

Ferroptosis, an iron-dependent cell death, is characterized by excessive lipid peroxidation, ultimately leading to membrane rupture. The process is triggered by iron accumulation, ROS generation, and the ensuing lipid peroxidation.<sup>11</sup> Our prior experiments verified that the increase in ROS and MDA prompted us to explore the level of intracellular iron ion accumulation. FerroOrange, a fluorescent probe, can effectively monitor the variations of Fe<sup>2+</sup> within cells. Upon binding with Fe<sup>2+</sup>, FerroOrange emits a persistent orange fluorescent signal. By using the FerroOrange probe, we found that cells under combined treatment exhibited a significant elevation in intracellular Fe<sup>2+</sup>. However, the supplementation of glutathione (GSH), a crucial component of the defense system against ROS accumulation, alleviated the accumulation of Fe<sup>2+</sup> (Figure 4A).

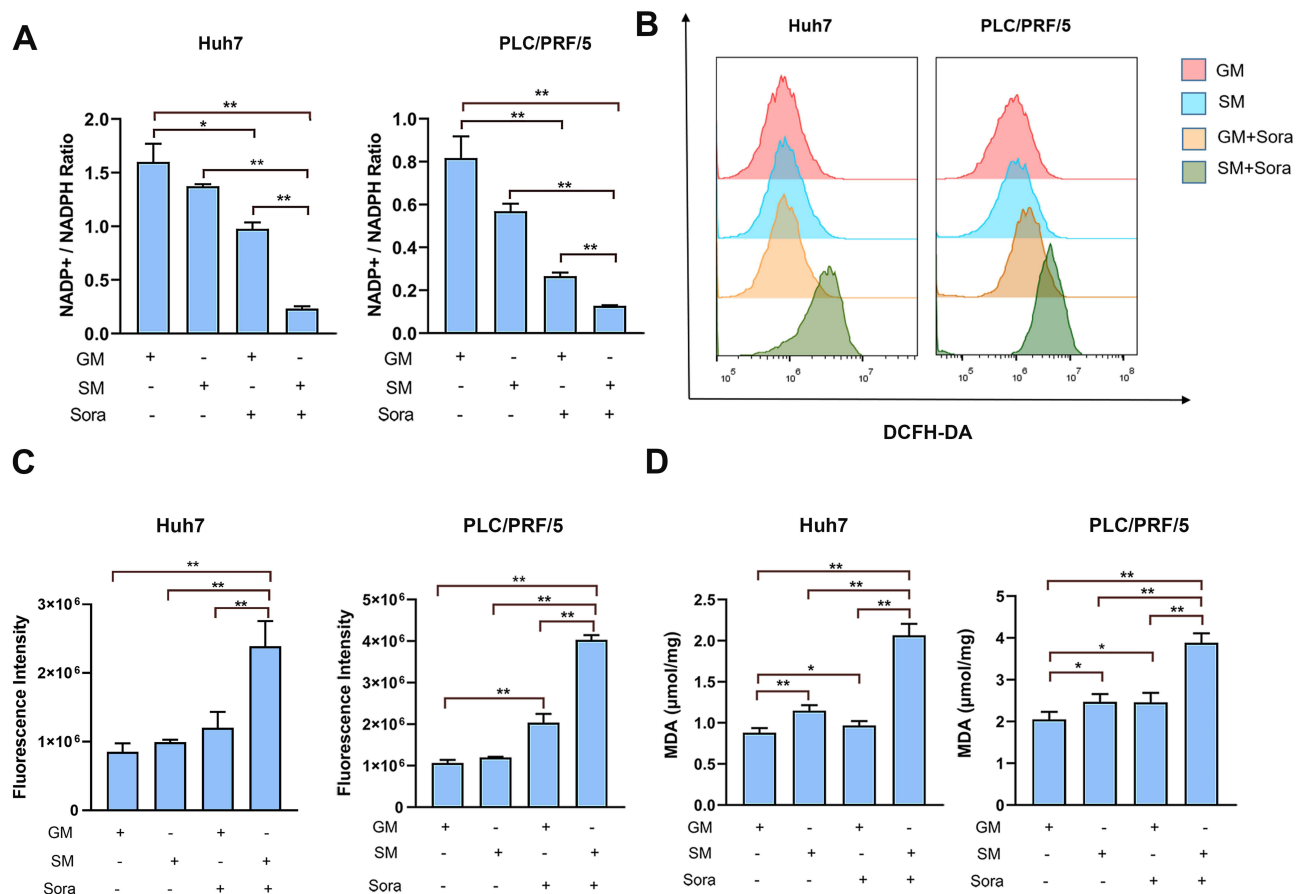


**Figure 3** The combination of nutrient restriction and Sorafenib disrupted the oxidative balance in HCC cells. **(A)** The NADP+/NADPH ratio significantly decreased by the combination treatment (mean ± SD, n = 6, \*p < 0.05; \*\*p < 0.01); **(B)** Cellular ROS levels were notably increased under the combination treatment; **(C)** Quantitative analysis showed a significant increase in cellular ROS levels (mean ± SD, n = 6, \*\*p < 0.01); **(D)** The cellular MDA content was significantly elevated by the combination treatment (mean ± SD, n = 6, \*p < 0.05; \*\*p < 0.01). Shown is a result from at least 3 independent experiments.

**Abbreviation:** MDA, malondialdehyde.

The C11-BODIPY probe is typically used to determine cellular lipid peroxidation. When a cell undergoes lipid peroxidation, the emitted fluorescence shifts from 590nm (FL2 channel) to 510nm (FL1 channel). By employing the C11-BODIPY probe, we further validated that the combination of Sorafenib and nutritional restriction significantly enhanced cellular lipid peroxidation, while GSH suppressed this enhancement in HCC cells (1.4-fold in Huh7,  $p < 0.01$ ; and 1.2-fold in PLC/PRF/5 cells,  $p < 0.05$ , Figure 4B and C). Recent studies have demonstrated that Sorafenib induces ferroptosis rather than apoptosis.<sup>28–30</sup> Basis on these findings, we conclude that nutrient restriction promotes Sorafenib-induced ferroptosis in HCC.

Ferroptosis can be triggered by either GSH depletion or the inactivation of Glutathione peroxidase 4 (GPX4).<sup>31</sup> GPX4 is the key molecule in the ferroptotic pathway, responsible for catalyzing GSH to convert lipid peroxides into lipid alcohols, thereby preventing the propagation of lipid peroxidation across the membrane. Nuclear factor erythroid 2-related factor 2 (NRF2) is a crucial transcription factor that maintains redox balance during oxidative stress. In response to ROS stress, NRF2 rapidly dissociates and translocates to the cell nucleus, activating the endogenous antioxidant factor heme oxygenase-1 (HO-1), which subsequently establishes the NRF2/HO-1 antioxidant defense system. However, the inactivation of antioxidant systems, such as NRF2/HO-1, can elevate oxidative stress, and increase iron accumulation, potentially leading to ferroptosis.

To further investigate the association of nutrient restriction, Sorafenib, and cell ferroptosis via the NRF2/HO-1/GPX4 axis in HCC cells, we utilized Western blot analysis in HCC cells. The results identified a significant reduction in the expression of these proteins in the combined treated cells. Nevertheless, the addition of GSH increased the expression of

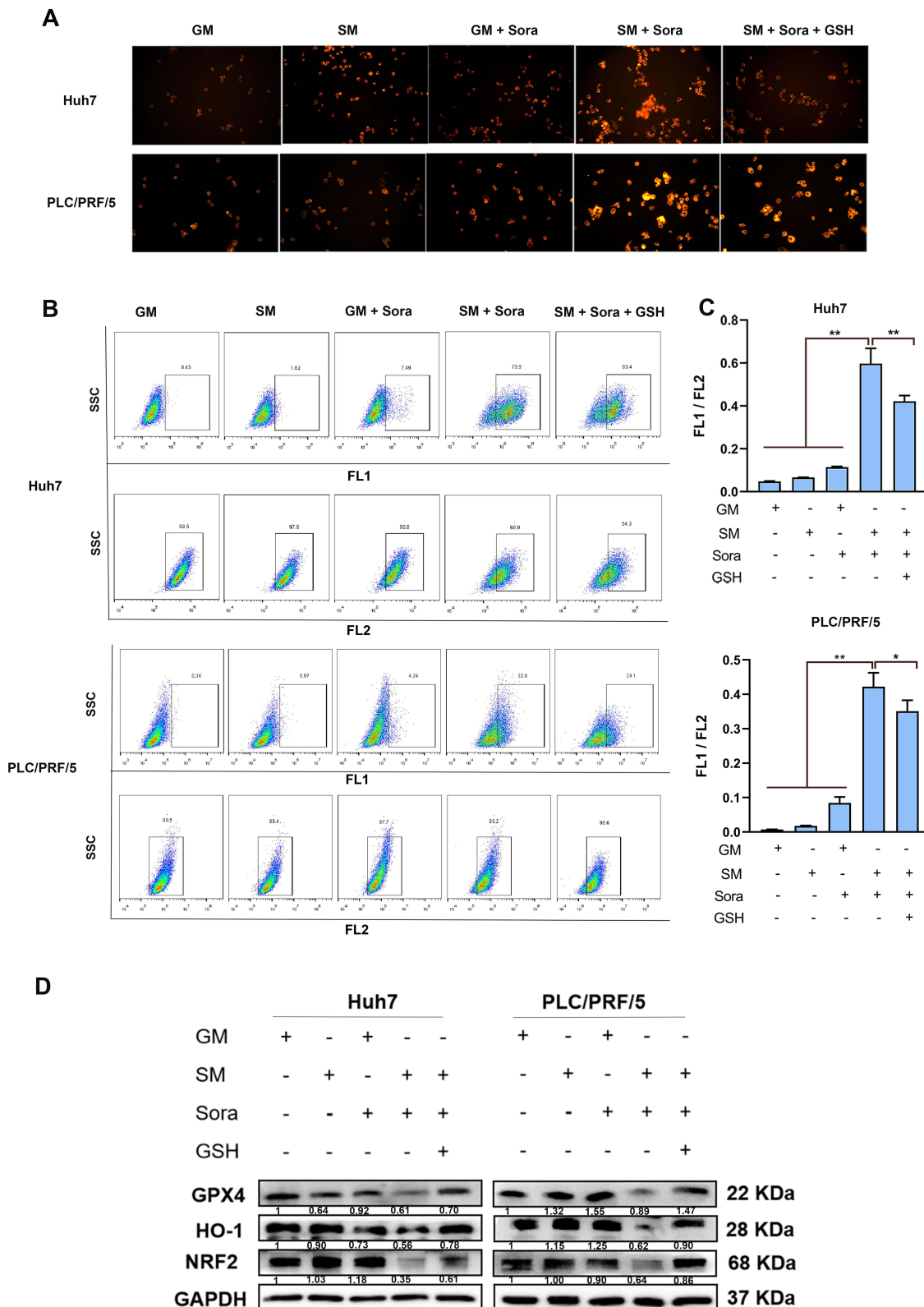


**Figure 4** Nutrient Restriction Enhanced the Efficacy of Sorafenib by Inducing Ferroptosis via the NRF2/HO-1/GPX4 Axis **(A)** The FerroOrange fluorescent probe was employed to assess intracellular Fe<sup>2+</sup> accumulation. Notably, the combination treatment resulted in a pronounced elevation of Fe<sup>2+</sup> levels within the cells, while GSH supplementation effectively attenuated this accumulation; **(B)** Utilizing the C11-BODIPY probe and FCM, a substantial increase in lipid peroxidation was observed in cells subjected to the combination treatment. **(C)** Quantification of FL1 (510nm)/FL2 (590nm) (mean ± SD, n = 6, \*p < 0.05; \*\*p < 0.01); **(D)** Western blot was used to assess the expression of proteins linked to the NRF2/HO-1/GPX4 axis.

**Abbreviations:** GSH, glutathione; FCM, flow cytometry.

these proteins (Figure 4D). These results suggest that nutrient restriction enhances the anti-tumor effect of Sorafenib by regulating the NRF2/HO-1/GPX4 axis.

## In vivo Therapeutic Validation of Intermittent Fasting Combined with Sorafenib

We further verified these result in animals. Tumor-bearing mice were randomly divided into four groups: the AL group, the IF group, the AL + Sora group, and the IF + Sora group (Figure 5A and B). Notably, a remarkable suppression of tumor growth was observed in the mice of the IF + Sora group (Figure 5C), along with a significant reduction in tumor weight (3.8-fold decrease vs AL group,  $p < 0.01$ ; 3.2-fold decrease vs AL + IF,  $p < 0.05$ ; group 1.9-fold decrease vs AL + Sora group,  $p < 0.05$ , Figure 5D and E). HE staining showed the largest necrotic patches in the tumors treated with IF + Sora (Figure 5F). These results demonstrate that nutrient restriction/intermittent fasting enhances the therapeutic efficacy of Sorafenib in xenograft tumors. Further validation via Western blot and IHC analysis of xenograft tumors indicated that the combination of intermittent fasting and Sorafenib reduced the levels of ferroptosis associated proteins (Figure 5G–I). These results suggest that nutrient restriction/intermittent fasting enhances the anti-tumor effect of Sorafenib by regulating the NRF2/HO-1/GPX4 axis.

## Discussion

Tumors depend on nutrients supplied by the host for their growth and survival. Dietary modifications of the host can alter nutrient availability within the tumor microenvironment, presenting a promising strategy for inhibiting tumor growth.<sup>32</sup> Recent preclinical models and early clinical studies have provided compelling evidence that certain dietary patterns play a powerful role in cancer prevention and treatment. These patterns work by preventing tumorigenesis, slowing tumor growth, and synergizing with a variety of anticancer therapies.<sup>6,33</sup> Despite promising results, the lack of robust mechanistic evidence and the limitations of large-scale clinical trials of nutritional therapeutics has resulted in dietary interventions being largely overlooked in the clinic, particularly in the context of cancer treatment.

Our findings reflects that combination therapy of nutrient restriction/intermittent fasting and Sorafenib creates synthetic lethality by targeting energy/redox systems, while monotherapies preserve metabolic thresholds. ATP levels dropped to 29–49% with combination vs 63–71% under monotherapies. Corresponding p-AMPK suggests combination therapy breaches critical ATP thresholds. Similarly, NADP+/NADPH ratios plummeted to 15–16% with combination vs 33–86% in monotherapies. Despite this, relative stable ROS and minimal lipid peroxidation confirm monotherapies maintain redox balance, while combination induces critical imbalance. Collectively, these findings support our hypothesis that combination therapy of nutrient restriction/intermittent fasting and Sorafenib creates a synthetic lethal metabolic bottleneck through targeting energy production and redox homeostasis. While our data demonstrate that nutrient restriction potently enhances Sorafenib-induced ferroptosis, prior reports indicate glucose deprivation acts synergistically independently of ferroptosis.<sup>34</sup> Notably, the latter study based this conclusion exclusively on ferrostatin-1 pretreatment (5 $\mu$ M, 30min) in HCC models. This apparent discrepancy may arise from two critical factors: (1) Limitations of ferroptosis inhibitors: the conclusion of ferroptosis independence relied solely on ferrostatin-1 pretreatment, which may not fully inhibit ferroptosis in HCC due to short duration and suboptimal concentration. (2) Metabolic specificity: our nutrient restriction model differ from glucose deprivation. Integrated metabolic stress depletes glutathione to induce ferroptosis, whereas glucose starvation primarily disrupts ATP/NADPH balance, activating mitophagy. Notably, emerging evidence indicates that autophagy activation can promote ferroptosis through molecular crosstalk.<sup>35</sup> Rapamycin, an autophagy inducer targeting mTOR, has been linked to tumor cell ferroptosis in several studies.<sup>36–38</sup> Further explorations is warranted to validate these regulatory mechanism in HCC.

Sorafenib is the standard medication for advanced HCC, and multiple studies have been conducted to identify effective combination strategies that can sensitize HCC to Sorafenib treatment.<sup>39–41</sup> Multiple recent studies confirm Sorafenib induces ferroptosis in HCC.<sup>42–45</sup> However, HCC is highly heterogeneous, a single combination regimen may only be beneficial for a small proportion of patients. In this study, we demonstrated that restricting nutrients enhances the anti-tumor efficacy of Sorafenib in HCC models by promoting cellular ferroptosis (Figure 6). Therefore, we propose that combining nutrient restriction/intermittent fasting with Sorafenib represents a potential approach that could benefit a broader range of HCC patients due to its low toxicity and affordability. In addition, our research provides evidence

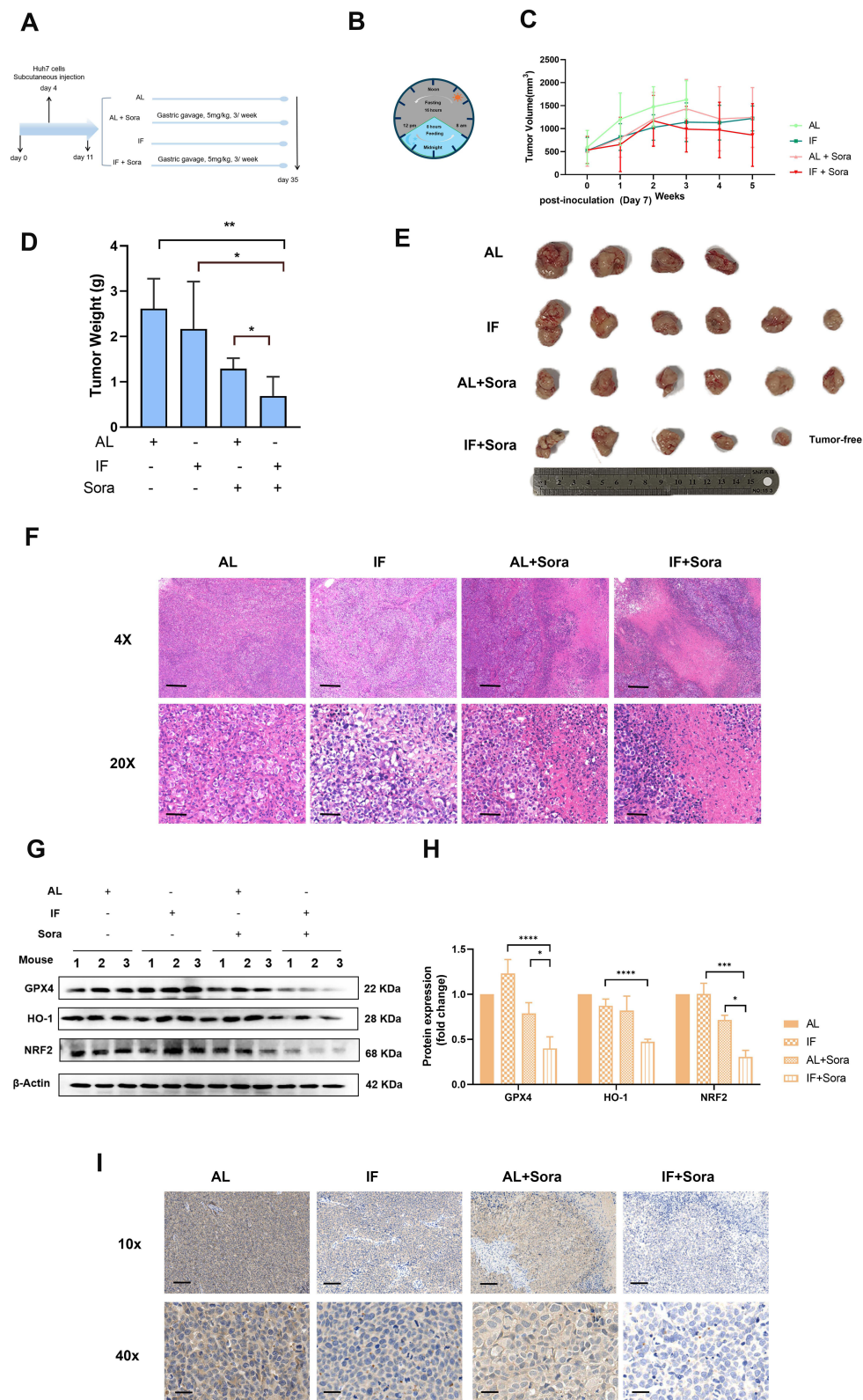


**Figure 5** Intermittent fasting enhanced the antitumor effect of Sorafenib *in vivo* by modulating the NRF2/HO-1/GPX4 axis. **(A)** Experimental scheme for mouse experiment; **(B)** Feeding schedule for IF mice; **(C)** Tumor volumes were monitored weekly (mean  $\pm$  SD,  $n = 6$ ); **(D)** Tumors were isolated and weighed after euthanasia (mean  $\pm$  SD,  $n = 6$ , \* $p < 0.05$ ; \*\* $p < 0.01$ ); **(E)** Tumor images of validation samples in mice; **(F)** HE staining of tumors (Scale bar: 240  $\mu\text{m}$  for 4X and 50  $\mu\text{m}$  for 20X); **(G)** Western blot revealed the expression of proteins linked to the NRF2/HO-1/GPX4 axis; **(H)** Quantification for the expression of NRF2/HO-1/GPX4 axis in xenograft tumors (mean  $\pm$  SD,  $n = 3$ , \* $p < 0.05$ ; \*\* $p < 0.001$ ; \*\*\* $p < 0.0001$ ); **(I)** Immunohistochemical staining of GPX4 in xenograft tumors (Scale bar: 100  $\mu\text{m}$  for 10X and 25  $\mu\text{m}$  for 40X). Shown is a result from at least 3 independent experiments.

**Abbreviations:** AL, ad libitum; IF, intermittent fasting; Sora, Sorafenib.

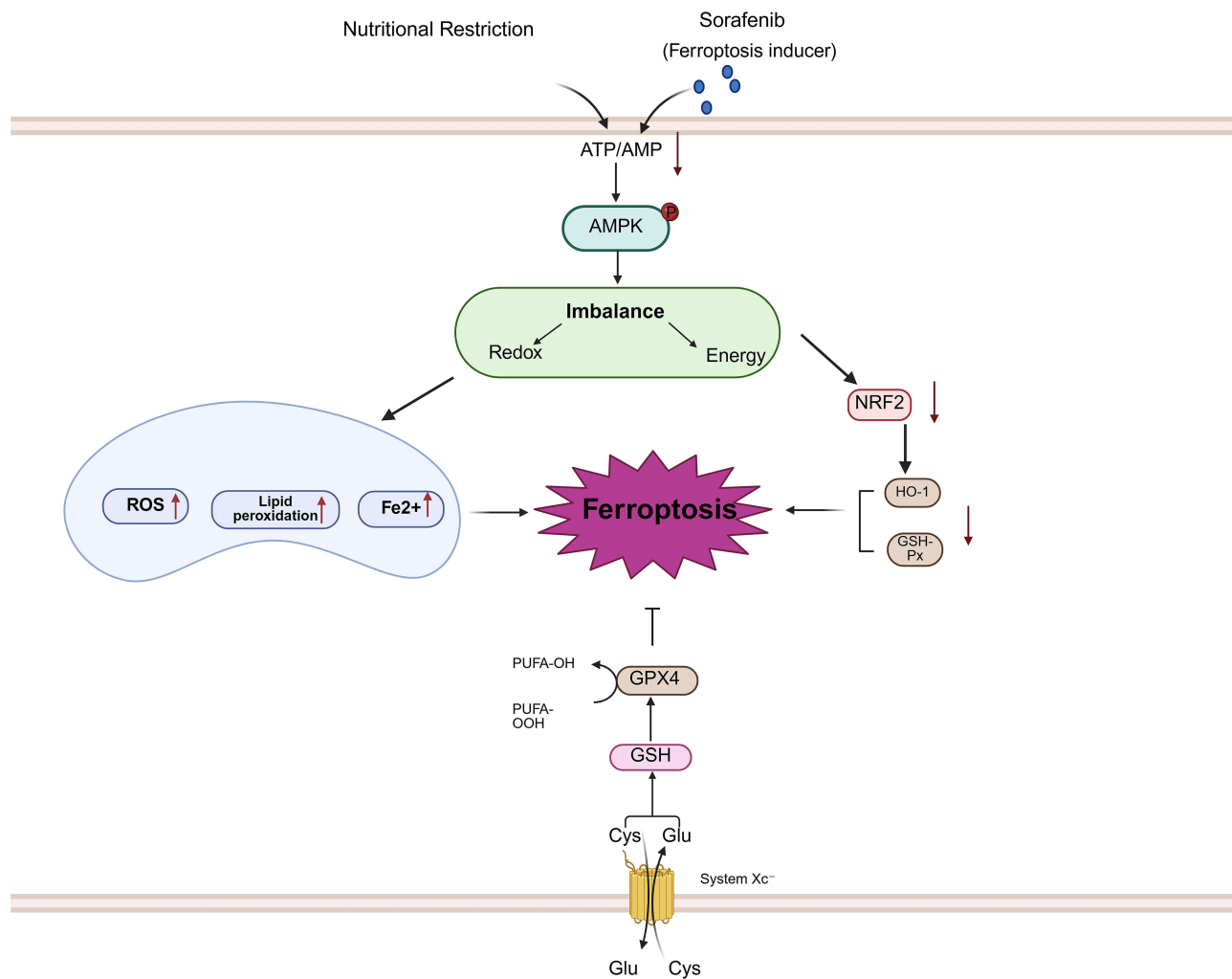


**Figure 6** Schematic summarizing the mechanism by which nutrient restriction enhances sorafenib-induced ferroptosis in HCC. Arrow denote increases (↑) or decreases (↓) in levels.

**Abbreviations:** ROS, reactive oxygen species; Fe<sup>2+</sup>, ferrous ion; ATP, adenosine triphosphate; AMP, adenosine monophosphate; NRF2, nuclear factor erythroid 2-related factor 2; HO-1, heme oxygenase-1; GSH-Px, glutathione peroxidase; GPX4, glutathione peroxidase 4.

supporting ferroptosis induction as a strategy to improve the effectiveness of Sorafenib in HCC treatment. Louandre et al reported that DFX, a potent iron chelator, offers protection to HCC cells against the cytotoxic effects of Sorafenib.<sup>29</sup> When administered at the low dose, Sorafenib predominantly induces oxidative stress by disrupting mitochondrial function and inhibiting SLC7A11, leading to a depletion of GSH.<sup>3</sup> Previous studies indicated that fasting improves the therapeutic efficacy of Sorafenib in HCC through a p53-dependent metabolic synergism,<sup>8</sup> and the combined approach of fasting and ferroptosis inducers notably promotes cell death in colorectal cancer.<sup>10</sup> In the present study, we found that nutrient restriction promoted Sorafenib-induced cell ferroptosis by generating excessive ROS and modulating the NRF2/HO-1/GPX4 axis. The NRF2/HO-1 axis, recognized for its critical function in reducing oxidative stress, holds a crucial position in the cellular defense system. By activating NRF2 and subsequently upregulating HO-1 and GPX4, oxidative stress can be reduced, preserving mitochondrial integrity and possibly averting mitochondrial dysfunction. Our results not only corroborate but also expand upon previous research, highlighting the significant role of intracellular iron stores, excessive ROS, and mitochondrial dysfunction in Sorafenib-induced cell death. These insights pave the way for new therapeutic strategies targeting HCC cells.

The therapeutic response to nutrient modulation in HCC is highly context-specific. Our findings show that moderate nutrient restriction synergizes with sorafenib by promoting ferroptosis. In contrast, other studies report that severe

nutrient deprivation can activate pro-survival pathways, leading to sorafenib resistance.<sup>46–48</sup> To reconcile these differences, we propose a “nutrient stress spectrum” framework: under severe starvation, cells activate emergency survival mechanisms that may induce cross-resistance; under the moderate restriction used in our model, cells undergo adaptive metabolic rewiring that increases susceptibility to therapy.

The implementation of fasting regimens into HCC therapy requires careful consideration of patient nutritional status. Classical fasting is often inappropriate in advanced HCC patients due to prevalent malnutrition. A feasible alternative is the use of Fasting-Mimicking Diets (FMDs), which provide essential nutrients while inducing a fasting-like metabolic state.<sup>7</sup> Future trials should implement rigorous monitoring of liver function, body composition, and quality of life.

Our data further prompt a pivotal question regarding the specificity of this chemosensitization effect: Is nutrient restriction mediated chemosensitization specific to sorafenib? We propose that the effect is not universal but mechanistically selective, depending on alignment between nutrient restriction-induced metabolic vulnerabilities (eg, impaired lipid peroxidation repair) and the drug’s primary cell-killing pathway. Thus, agents whose action involves or can be co-opted to induce ferroptosis are the most promising candidates for synergy with nutrient restriction, a concept supported by growing literature on the selective enhancement of oxidative stress-based therapies by dietary interventions.<sup>10,49</sup>

Two main limitations should be noted. First, the analysis is centered on the glutathione-GPX4 axis, whereas ferroptosis is regulated by a broader network (eg, ACSL4, PTGS2), future studies should integrate these markers. Second, the athymic nude mouse model was chosen to isolate direct tumoricidal effects, yet it cannot assess adaptive immune responses, necessitating future validation in immunocompetent models.

In summary, this study demonstrated that nutrient restriction combined with Sorafenib altered the energy metabolism, and disrupted redox balance in HCC cells. Additionally, this kind of combination modulates the NRF2/HO-1/GPX4 antioxidant axis, ultimately augments Sorafenib-induced ferroptosis. These results emphasize the potential of dietary adjustments in advancing cancer research and treatment. Furthermore, the study emphasizes the importance of considering patients’ dietary habits and nutritional status during clinical medication administration.

## Data Sharing Statement

All the data generated or analyzed in this study are included either in this manuscript or in the [supplementary information file](#).

## Ethical Compliance Statement

All experimental procedures involving animals were conducted in strict accordance with the Animal Research: Reporting of In Vivo Experiments (ARRIVE) guidelines. Specific pathogen-free (SPF) male Balb/c nude mice were procured from Slack Laboratory Animal Co., Ltd. (Production License: SCXK [Hu] 2017-0005; Quality Certificate: 20220004046355). The animal research protocol was approved (Approval code: IACUC-20190108; Approval Date: March 2019) by the Institutional Animal Care and Use Committee (IACUC) of Zhejiang Sci-Tech University, China.

## Consent for Publication

All the authors agree to the publication of the results of the present manuscript.

## Author Contributions

All authors made a significant contribution to the work reported, whether that is in the conception, study design, execution, acquisition of data, analysis and interpretation, or in all these areas; took part in drafting, revising or critically reviewing the article; gave final approval of the version to be published; have agreed on the journal to which the article has been submitted; and agree to be accountable for all aspects of the work.

## Funding

Supported by National Natural Science Foundation of China (No. 81972281) for Kan Chen, and Medical Science and Technology Project of Zhejiang Province for Chong Jin (No. 2025KY454).

## Disclosure

The authors report no conflicts of interests in this work.

## References

- Llovet JM, Pinyol R, Kelley RK, et al. Molecular pathogenesis and systemic therapies for hepatocellular carcinoma. *Nat Cancer*. 2022;3(4):386–401. doi:10.1038/s43018-022-00357-2
- Galle PR, Forner A, Llovet JM, et al. EASL clinical practice guidelines: management of hepatocellular carcinoma. *J Hepatol*. 2018;69(1):182–236. doi:10.1016/j.jhep.2018.03.019
- Li ZJ, Dai HQ, Huang XW, et al. Artesunate synergizes with sorafenib to induce ferroptosis in hepatocellular carcinoma. *Acta Pharmacol Sin*. 2021;42(2):301–310. doi:10.1038/s41401-020-0478-3
- Llovet JM, Ricci S, Mazzaferro V, et al. Sorafenib in advanced hepatocellular carcinoma. *N Engl J Med*. 2008;359(4):378–390. doi:10.1056/NEJMoa0708857
- Yang Z, Song L, Chen H, Chen Y, Xie Y, Xie J. Exploring the potential anticancer effects of *Lobelia chinensis* Lour in liver cancer via multiomics analysis. *Med Res*. 2025;1(3):483–488. doi:10.1002/mdr2.70025
- Taylor SR, Falcone JN, Cantley LC, Goncalves MD. Developing dietary interventions as therapy for cancer. *Nat Rev Cancer*. 2022;22(8):452–466. doi:10.1038/s41568-022-00485-y
- Nencioni A, Caffà I, Cortellino S, Longo VD. Fasting and cancer: molecular mechanisms and clinical application. *Nat Rev Cancer*. 2018;18(11):707–719. doi:10.1038/s41568-018-0061-0
- Krstic J, Reinisch I, Schindlmaier K, et al. Fasting improves therapeutic response in hepatocellular carcinoma through p53-dependent metabolic synergism. *Sci Adv*. 2022;8(3):eabh2635. doi:10.1126/sciadv.abh2635
- Kazmirczak F, Hartweck LM, Vogel NT, et al. Intermittent fasting activates AMP-kinase to restructure right ventricular lipid metabolism and microtubules. *JACC Basic Transl Sci*. 2023;8(3):239–254. doi:10.1016/j.jacbs.2022.12.001
- Liu X, Peng S, Tang G, et al. Fasting-mimicking diet synergizes with ferroptosis against quiescent, chemotherapy-resistant cells. *EBioMedicine*. 2023;90:104496. doi:10.1016/j.ebiom.2023.104496
- Mao L, Zhao T, Song Y, et al. The emerging role of ferroptosis in non-cancer liver diseases: hype or increasing hope? *Cell Death Dis*. 2020;11(7):518. doi:10.1038/s41419-020-2732-5
- Lyublinskaya OG, Ivanova JS, Pugovkina NA, et al. Redox environment in stem and differentiated cells: a quantitative approach. *Redox Biol*. 2017;12:758–769. doi:10.1016/j.redox.2017.04.016
- Gedaly R, Angulo P, Hundley J, et al. PI-103 and sorafenib inhibit hepatocellular carcinoma cell proliferation by blocking Ras/Raf/MAPK and PI3K/AKT/mTOR pathways. *Anticancer Res*. 2010;30(12):4951–4958.
- Wilhelm SM, Carter C, Tang L, et al. BAY 43-9006 exhibits broad spectrum oral antitumor activity and targets the RAF/MEK/ERK pathway and receptor tyrosine kinases involved in tumor progression and angiogenesis. *Cancer Res*. 2004;64(19):7099–7109. doi:10.1158/0008-5472.Can-04-1443
- Yang M, Wu X, Hu J, et al. COMMD10 inhibits HIF1 $\alpha$ /CP loop to enhance ferroptosis and radiosensitivity by disrupting Cu-Fe balance in hepatocellular carcinoma. *J Hepatol*. 2022;76(5):1138–1150. doi:10.1016/j.jhep.2022.01.009
- Zhong Z, Umemura A, Sanchez-Lopez E, et al. NF- $\kappa$ B restricts inflammasome activation via elimination of damaged mitochondria. *Cell*. 2016;164(5):896–910. doi:10.1016/j.cell.2015.12.057
- Maeda S, Kamata H, Luo JL, Leffert H, Karin M. IKK $\beta$  couples hepatocyte death to cytokine-driven compensatory proliferation that promotes chemical hepatocarcinogenesis. *Cell*. 2005;121(7):977–990. doi:10.1016/j.cell.2005.04.014
- He F, Zhang P, Liu J, et al. ATF4 suppresses hepatocarcinogenesis by inducing SLC7A11 (xCT) to block stress-related ferroptosis. *J Hepatol*. 2023;79(2):362–377. doi:10.1016/j.jhep.2023.03.016
- Zhang S, Song X, Cao D, et al. Pan-mTOR inhibitor MLN0128 is effective against intrahepatic cholangiocarcinoma in mice. *J Hepatol*. 2017;67(6):1194–1203. doi:10.1016/j.jhep.2017.07.006
- Yang R, Gao W, Wang Z, et al. Polyphyllin I induced ferroptosis to suppress the progression of hepatocellular carcinoma through activation of the mitochondrial dysfunction via Nrf2/HO-1/GPX4 axis. *Phytomedicine*. 2024;122:155135. doi:10.1016/j.phymed.2023.155135
- Zhang Y, Dong Y, Chen S, et al. Targeting NAT10 inhibits hepatocarcinogenesis via ac4C-Mediated SMAD3 mRNA stability. *Exploration*. 2025;5(6):20250075. doi:10.1002/exp.20250075
- Dixon SJ, Patel DN, Welsch M, et al. Pharmacological inhibition of cystine-glutamate exchange induces endoplasmic reticulum stress and ferroptosis. *Elife*. 2014;3:e02523. doi:10.7554/eLife.02523
- van Veelen W, Korsche SE, van de Laar L, Peppelenbosch MP. The long and winding road to rational treatment of cancer associated with LKB1/AMPK/TSC/mTORC1 signaling. *Oncogene*. 2011;30(20):2289–2303. doi:10.1038/ncr.2010.630
- Mihaylova MM, Shaw RJ. The AMPK signalling pathway coordinates cell growth, autophagy and metabolism. *Nat Cell Biol*. 2011;13(9):1016–1023. doi:10.1038/ncb2329
- Koju N, Qin ZH, Sheng R. Reduced nicotinamide adenine dinucleotide phosphate in redox balance and diseases: a friend or foe? *Acta Pharmacol Sin*. 2022;43(8):1889–1904. doi:10.1038/s41401-021-00838-7
- Nakamura H, Takada K. Reactive oxygen species in cancer: current findings and future directions. *Cancer Sci*. 2021;112(10):3945–3952. doi:10.1111/cas.15068
- Xie Q, Sun Y, Xu H, et al. Ferrostatin-1 improves BMSC survival by inhibiting ferroptosis. *Arch Biochem Biophys*. 2023;736:109535. doi:10.1016/j.abb.2023.109535
- Sehm T, Rauh M, Wiendieck K, Buchfelder M, Eyüpoglu IY, Savaskan NE. Temozolomide toxicity operates in a xCT/SLC7a11 dependent manner and is fostered by ferroptosis. *Oncotarget*. 2016;7(46):74630–74647. doi:10.18632/oncotarget.11858
- Louandre C, Ezzoukry Z, Godin C, et al. Iron-dependent cell death of hepatocellular carcinoma cells exposed to sorafenib. *Int J Cancer*. 2013;133(7):1732–1742. doi:10.1002/ijc.28159

30. Sun X, Niu X, Chen R, et al. Metallothionein-1G facilitates sorafenib resistance through inhibition of ferroptosis. *Hepatology*. 2016;64(2):488–500. doi:10.1002/hep.28574
31. Zhao T, Yu Z, Zhou L, et al. Regulating Nrf2-GPx4 axis by bicyclol can prevent ferroptosis in carbon tetrachloride-induced acute liver injury in mice. *Cell Death Discov*. 2022;8(1):380. doi:10.1038/s41420-022-01173-4
32. Kanarek N, Petrova B, Sabatini DM. Dietary modifications for enhanced cancer therapy. *Nature*. 2020;579(7800):507–517. doi:10.1038/s41586-020-2124-0
33. Martínez-Garay C, Djouder N. Dietary interventions and precision nutrition in cancer therapy. *Trends Mol Med*. 2023;29(7):489–511. doi:10.1016/j.molmed.2023.04.004
34. Zhou J, Feng J, Wu Y, et al. Simultaneous treatment with sorafenib and glucose restriction inhibits hepatocellular carcinoma in vitro and in vivo by impairing SIAH1-mediated mitophagy. *Exp Mol Med*. 2022;54(11):2007–2021. doi:10.1038/s12276-022-00878-x
35. Liao C, He Y, Luo X, Deng G. Ferroptosis: insight into the treatment of hepatocellular carcinoma. *Cancer Cell Int*. 2024;24(1):376. doi:10.1186/s12935-024-03559-z
36. Sun Y, Berleth N, Wu W, et al. Fin56-induced ferroptosis is supported by autophagy-mediated GPX4 degradation and functions synergistically with mTOR inhibition to kill bladder cancer cells. *Cell Death Dis*. 2021;12(11):1028. doi:10.1038/s41419-021-04306-2
37. Zhang L, Liu W, Liu F, et al. IMCA induces ferroptosis mediated by SLC7A11 through the AMPK/mTOR pathway in colorectal cancer. *Oxid Med Cell Longev*. 2020;2020:1675613. doi:10.1155/2020/1675613
38. Li HW, Liu MB, Jiang X, et al. GALNT14 regulates ferroptosis and apoptosis of ovarian cancer through the EGFR/mTOR pathway. *Future Oncol*. 2022;18(2):149–161. doi:10.2217/fo-2021-0883
39. Faivre S, Rimassa L, Finn RS. Molecular therapies for HCC: looking outside the box. *J Hepatol*. 2020;72(2):342–352. doi:10.1016/j.jhep.2019.09.010
40. Jung DH, Tak E, Hwang S, et al. Antitumor effect of sorafenib and mammalian target of rapamycin inhibitor in liver transplantation recipients with hepatocellular carcinoma recurrence. *Liver Transpl*. 2018;24(7):932–945. doi:10.1002/lt.25191
41. Lin CH, Elkholy KH, Wani NA, et al. Ibrutinib potentiates antihepatocarcinogenic efficacy of sorafenib by targeting EGFR in tumor cells and BTK in immune cells in the stroma. *Mol Cancer Ther*. 2020;19(2):384–396. doi:10.1158/1535-7163.Mct-19-0135
42. Liu X, Zhang F, Fan Y, Qiu C, Wang K. MCM4 potentiates evasion of hepatocellular carcinoma from sorafenib-induced ferroptosis through Nrf2 signaling pathway. *Int Immunopharmacol*. 2024;142(Pt A):113107. doi:10.1016/j.intimp.2024.113107
43. Ma S, Xie F, Wen X, et al. GSTA1/CTNBN1 axis facilitates sorafenib resistance via suppressing ferroptosis in hepatocellular carcinoma. *Pharmacol Res*. 2024;210:107490. doi:10.1016/j.phrs.2024.107490
44. Gao S, Fan L, Wang H, et al. NCOA5 induces sorafenib resistance in hepatocellular carcinoma by inhibiting ferroptosis. *Cell Death Discov*. 2025;11(1):215. doi:10.1038/s41420-025-02473-1
45. Yin R, Tao Y, Han J, et al. STOML2 inhibits sorafenib-induced ferroptosis in hepatocellular carcinoma via p-AKT signaling pathway. *Am J Cancer Res*. 2025;15(4):1614–1628. doi:10.62347/sutj3506
46. Luo T, Fu J, Xu A, et al. PSMD10/gankyrin induces autophagy to promote tumor progression through cytoplasmic interaction with ATG7 and nuclear transactivation of ATG7 expression. *Autophagy*. 2016;12(8):1355–1371. doi:10.1080/15548627.2015.1034405
47. Loong JH, Wong TL, Tong M, et al. Glucose deprivation-induced aberrant FUT1-mediated fucosylation drives cancer stemness in hepatocellular carcinoma. *J Clin Invest*. 2021;131(11):e143377. doi:10.1172/jci143377
48. Lo Re O, Panebianco C, Porto S, et al. Fasting inhibits hepatic stellate cells activation and potentiates anti-cancer activity of Sorafenib in hepatocellular cancer cells. *J Cell Physiol*. 2018;233(2):1202–1212. doi:10.1002/jcp.25987
49. Wu Y, Zhang Z, Ren M, et al. Metformin induces apoptosis and ferroptosis of ovarian cancer cells under energy stress conditions. *Cells*. 2025;14(3):213. doi:10.3390/cells14030213

Journal of Hepatocellular Carcinoma

Publish your work in this journal

The Journal of Hepatocellular Carcinoma is an international, peer-reviewed, open access journal that offers a platform for the dissemination and study of clinical, translational and basic research findings in this rapidly developing field. Development in areas including, but not limited to, epidemiology, vaccination, hepatitis therapy, pathology and molecular tumor classification and prognostication are all considered for publication. The manuscript management system is completely online and includes a very quick and fair peer-review system, which is all easy to use. Visit <http://www.dovepress.com/testimonials.php> to read real quotes from published authors.

Submit your manuscript here: <https://www.dovepress.com/journal-of-hepatocellular-carcinoma-journal>

**Dovepress**  
Taylor & Francis Group